2015 International Conference on Unmanned Aircraft Systems (ICUAS)
Denver Marriott Tech Center
Denver, Colorado, USA, June 9-12, 2015

A Detailed Field Study of Direct Correlations Between Ground Truth Crop Water Stress and Normalized Difference Vegetation Index (NDVI) from Small Unmanned Aerial System (sUAS)

Tiebiao Zhao, Brandon Stark, YangQuan Chen*, Andrew L. Ray and David Doll

Abstract— **Aerial images with high spatial resolution and high temporal resolution were used to detect water stress based on canopy level normalized difference vegetation index (NDVI). We attempted to determine the correlation between stem water potential (SWP) and canopy NDVI with and without shade. Results indicated that removing the shade from the canopy improved the correlation between the NDVI of canopy and SWP with coefficient of determination (R^2) from 0.001 to 0.0052. We further compared SWP and the NDVI of the canopy without shade over a period of one week to four weeks. The correlation between NDVI with SWP was highest in the time range of three weeks. However, both cases show that there is no obvious relationship between NDVI of canopy and SWP. Therefore, canopy level NDVI does not indicate water stress. Further research is needed beyond pretty pictures.**

Index Terms— **NDVI (normalized difference vegetation index), crop water stress, SWP (stem water potential), crop canopy**

I. Introduction

Water is a critical factor in agriculture. Plants experience water stress when evaporative demand exceeds the water supply from the soil [1]. Even short-term water deficits may affect growth processes [2]. Water stress causes stomatal closure, prevents the uptake of carbon dioxide along with reducing water loss, and alters the color and temperature of leaves[3]. Plant species vary in water use and their response to water stress. A mature almond orchard for example, though a drought tolerant species [4], [5], can exhibit an evapotranspiration rate 50% greater than that of cotton [6], [7]. Water stress can seriously reduce the productive yield of almond trees [8], [9], [10]. As shown in Table I, there were four groups in the experiment treated with water of 40 in, 10 in, 5 in and 0 in. Compared with the yield under water treatment 40 in, the yield under treatment 10 in was 15% less. Further, the yield reduction reached up to 53% less if the water treatment is 0 in.

Water is a limited resource. As a major user of ground and surface water, agriculture accounts for about 80 percent of total consumptive water usage and up to 90 percent in many Western states (USDA). Therefore, water scarcity is a major limiting factor to irrigated agriculture in many areas [21]. In California, 58% of the state was considered to be in a severe drought [11], and 40 % percent of the state is in an 'exceptional drought' [12]. Consequently, it is important to improve irrigation scheduling to increase water usage efficiency. This has helped spurn considerable research on water stress detection. In [14], plant movement was used to detect water stress with machine vision, a method that is readily disrupted by wind. The photochemical reflectance index(PRI), which detects changes in xanthophylls pigment composition related to the de-epoxidation state of the xanthophyll cycle, has also been proposed to estimate water deficit in [15], [24]. Another method is based on thermal aerial imagery, which has been used as an indicator according to the inverse relation between canopy temperature and stomatal conductance [17], [16], [23], [25]. Near-infrared(NIR) has been proven capable of indicating crop physiological status [18], [20], [22].

However, most of these vegetation indices either focus on plant leaves [20], or are discussed based on data only within a few days [23], or are based on satellite images and which are inadequate for detecting water stress on single trees due to low spatial resolution. In this study, we examined whether images of high spatial (less than 2 centimeters) and temporal resolution (once a week) for canopy level normalized difference vegetation index (NDVI) is suitable for detecting water stress in an orchard setting.

TABLE I
Effects of irrigation treatment in almond trees [10]

Irrigation rate (in)	Yield (lbs/ac)	Nut size (g/nut)	Nuts (#/tree)
40	2224	1.16	7650
10	1890	1.04	7140
5	2020	0.97	7330
0	1030	0.72	5240

II. Materials and methods

A. Study site

The study was carried out between August and October, 2014 in a mature, commercial almond orchard of 80 acres, in Merced County, California (Fig. 1).

Tiebiao Zhao, Brandon Stark,and YangQuan Chen are with Mechatronics, Embedded Systems and Automation Lab, University of California, Merced, CA 95343, USA. Email:(tzhao3, bstark2, ychen53@ucmerced.edu). Andrew Ray and David Doll are with The Division of Agriculture and Natural Resources (ANR) of University of California (UCANR), Cooperative Extension (UCCE) Merced County, 2145 Wardrobe Avenue, Merced, CA 95341-6445.

*Corresponding author. Email: ychen53@ucmerced.edu, T: 209-228-4672, F: 209-228-4047, W: http://mechatronics.ucmerced.edu

978-1-4799-6009-5/15/$31.00 ©2015 IEEE

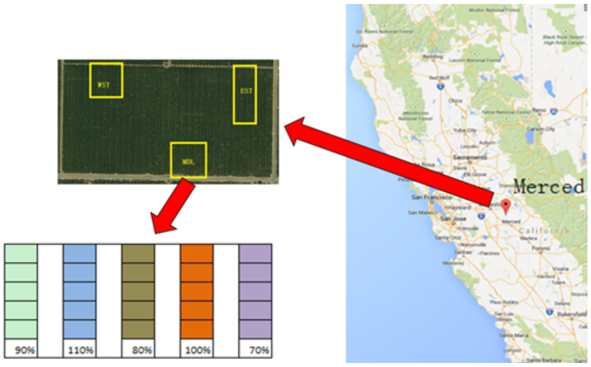

Fig. 1. Field site description

Fig. 3. Sprinklers in the ground truthing field

The orchard was established 15 years prior on a site in the field composed with Rocklin loam and Greenfield sandy. The orchard consists of the almond (Prunus dulcis) varieties 'Nonpareil', 'Carmel', and 'Monterey' planted on Lovell peach rootstock at a 5.5 m$\times$6.1m. Beginning in 2013, a range of different water application rate treatments were imposed on the orchard as part of a larger study to develop a water production function equation. In each of three experimental blocks, three rows of eighteen trees (Fig. 2) received one of five experimental treatments, an amount of irrigation water equivalent to 70%, 80%, 90%, 100%, or 110% of crop evapotranspiration (ET_c). The crop evapotranspiration is defined as the evapotranspiration from crops with optimum treatment under the given climatic conditions [27]. It is calculated according to

$$ET_c = K_c * ET_o \tag{1}$$

where ET_o is the evapotranspiration rate from a reference surface and K_c crop coefficients is the ratio of ET_c/ET_o. Trees are irrigated using one Supernet microsprinkler (Netafim) per tree (Fig. 3).

B. Field measurement

To determine the effects of irrigation treatments on tree water stress, stem water potential (SWP) is measured using a pressure chamber following standard procedures [28]. SWP is a sensitive indicator of water stress. To obtain the correct measurement, the leaf near the trunk is enclosed with aluminum foil for about 30 minutes to make sure leaf water potential matches with that of the stem or branches. Compared with the other indirect methods, such as soil water content or weather related measurements, SWP provides accurate information to help inform irrigation scheduling. However, the method is labor intensive and time consuming, since it requires twice visit to the sample tree and a certain amount of time for the sample leaves balancing water-potential gradient, which limits the amount of measurements that can be made per day. Following the concept that matching the water potential between leaves and stems by covering the leaves and eliminating the disturbances caused by stomata openings, a simplified method is proposed by Goldhamer and Fereres [19]. It has been proved that shaded leaves in the dense orchard have very low transpiration and are well related with water potential with the stems ($R^2 = 0.94$), i.e., these leaves are ready to be measured without being covered foils for a while. SWP was measured simultaneously as the flight. The sample tree lies in the middle of each section, equipped with a soil moisture probe, marked by red circle in Fig. 2.

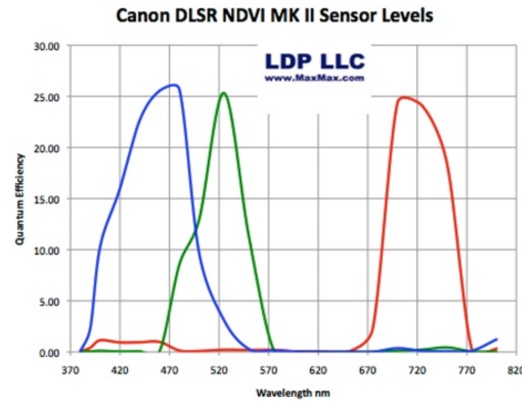

Fig. 4. Band set configuration of near-infrared camera

TABLE II
PARAMETERS OF COTS MULTISPECTRAL CAMERAS

Camera	ELPH110HS
FOV (horiz,degree)	71.22
FOV (vert,degree)	56.49
Focal length (mm)	4.3
CCD-width (mm)	6.16
CCD-height (mm)	4.62

C. Aerial imagery

Two COTS (Commercial-off-the-shelve) cameras (Canon, ELPH110HS, Japan) were flown from August to October, 2014, of which one is configured to detect three bands red, green, blue (RGB), and another configured to detect near-infrared(NIR), green, blue. The ELPH110HS has a resolution of 4608×3459 pixels with 24 bit radiometric resolution and has a focal length 4.3mm. More detail specifications are listed in Table II.

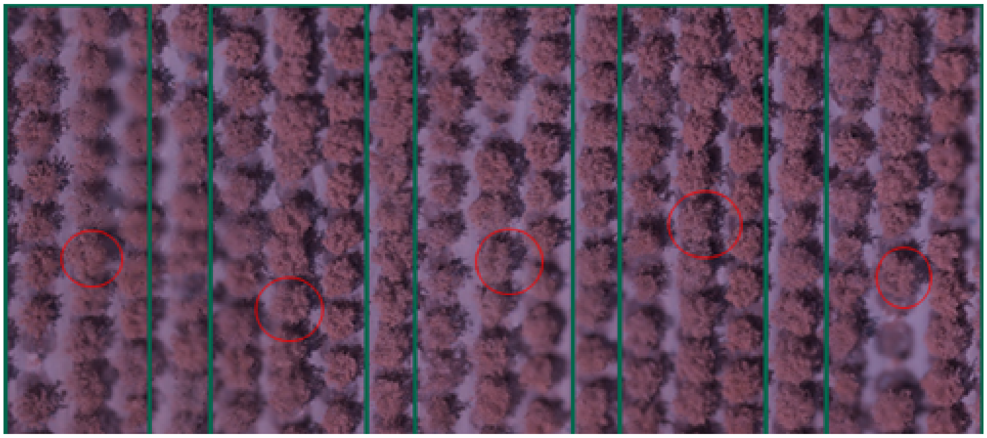

Fig. 2. Overview of one test block

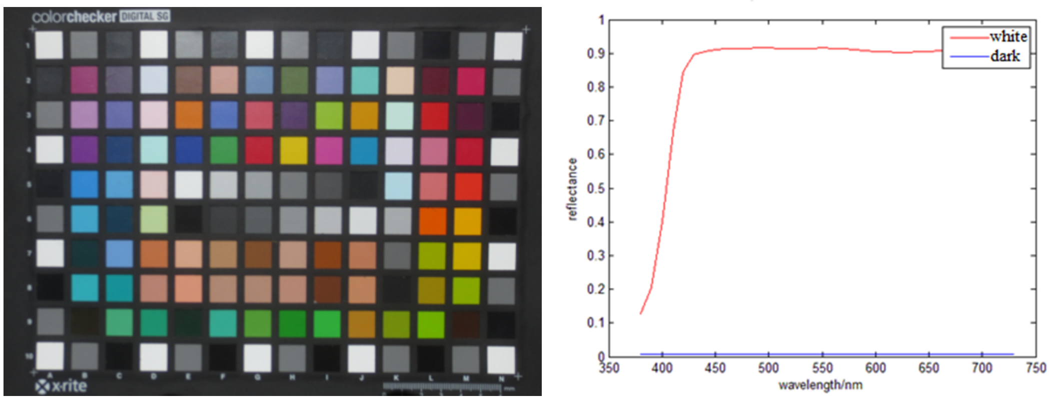

Fig. 5. Color checker and reflectance of white and dark spot

The RGB (Canon, ELPH110HS, Japan) camera is converted to the NIR camera by LDP, LLC, USA and its band sets are centered at 430nm, 530nm and 700 nm with the quantum efficiency shown in Fig. 4.

These cameras support Cannon Hack Development Kit (CHDK), which enables the autopilot to trigger cameras as the script programmed, and hence synchronizes the image with GPS and attitude log from the plane. Since it is difficult to discern differences among individual trees, it is difficult to align the images without the GPS information. Flight campaigns were conducted on 1:00 pm every Thursday at 60m altitude, yielding a ground spatial resolution of 1.87cm. The trigger distance for shooting was 16 m to generate vertical overlap up to 75%.

The raw data digital number (DN) value is converted to reflectance by an empirical method [26]. Before the flight, an image of color checker (Fig. 5) was taken, where there are perfect dark (DN_D) and white (DN_W) reference spots. Then a DN value can be converted to a reflectance using

$$\rho_\lambda = \frac{DN - DN_D}{DN_W - DN_D}. \quad (2)$$

The reflectance of white and dark spots on the color checker are shown in Fig. 5. It is very critical to take pictures of the color checker immediately prior to the flight campaign, otherwise the solar angle and light intensity will change and the conversion will not be accurate, as shown by five week time series. Table III shows that the DN values of dark and white spots exhibit considerable variability under different weather conditions, though all missions were conducted at the same time of day (1:00 pm). Here, the DN of dark spot and white spot is determined by the point located in the central part of its histogram, as shown in Figs. 6 and 7.

TABLE III
DN VALUE OF REFERENCE SPOT

Date	DN of dark spot		DN of white spot	
	Near infrared	Blue	Near infrared	Blue
Aug.13,2014	30	48	197	254
Aug.20,2014	31	78	223	254
Aug.27,2014	18	39	221	254
Sep.7, 2014	15	29	220	254
Sep.11,2014	24	44	254	254

Since there are little visual differences among trees, it was difficult to locate the sample tree, from which SWP was measured from a single image. Therefore, all of the obtained aerial images were stitched together to generate an orthophoto then the SWP sampled trees were cropped manually by placing ground point in Photoscan (AgiSoft LLC, Russia). Only the images in the most nadir footprint

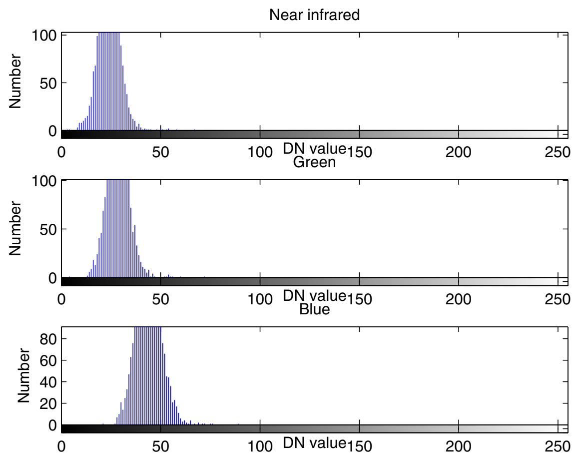

Fig. 6. Histogram of dark spot

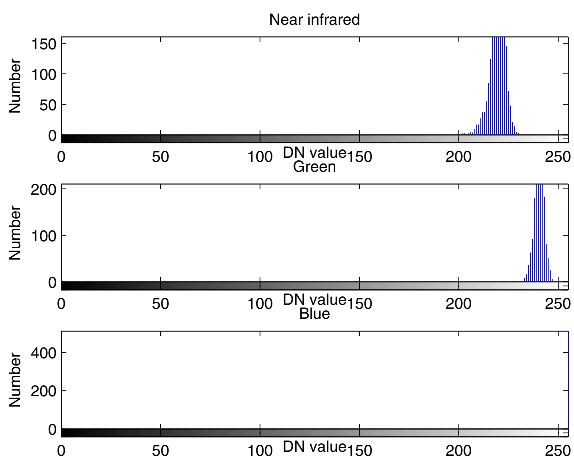

Fig. 7. Histogram of white spot

were considered for further processing. In total, images from 5 campaigns were processed for analysis. For each image of the individual tree, as shown in Fig. 9(a), first the shade and soil around the canopy was cut away as shown in Fig. 9(b), then only the region with the NDVI index value lying between 0.2 and 0.8 was recognized as region of interest of the canopy, while the other region is shaded crown, marked in white in Fig. 9(c). Finally, the canopy level NDVI was obtained by averaging NDVI among the region of interest of canopy.

In this paper, NDVI is calculated following the method (3), where the blue band is used as equally as red band, ρ_{NIR} stands for the reflectance of object in NIR band and ρ_B stands for the reflectance in blue band. This was possible because the imager was only 60 m from the ground and the atmosphere scattering would not have a significant effect on the vegetation index in blue band. Further, the technique generates better registration accuracy from the optical Bayer filter between the NIR and the blue bands than the method

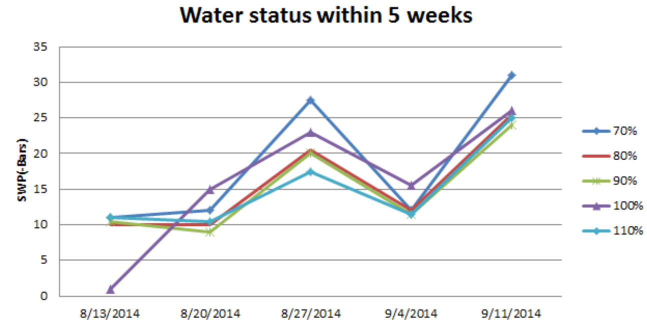

Fig. 8. Stem water potential within 5 weeks

using ground control points.

$$NDVI = \frac{\rho_{NIR} - \rho_B}{\rho_{NIR} + \rho_B}. \tag{3}$$

III. Results and Discussions

As shown in Fig. 8, the water stress levels were not parallel, i.e., the trees treated with more water were not always under less water stress than that treated with less water. Because the evapotranspiration of these trees were not the same, it is possible that these trees were facing different stresses even under the same irrigation frequency and different levels of irrigation.

The above presented data used for analysis is from the flight campaigns conducted each Thursday at 1:00 pm from Aug. 13 to Sep. 11 in 2014. The images were taken right after the SWP measurements were taken. We examined the relationship between canopy level NDVI and SWP with correlation analysis. Two different cases were compared: NDVI of the canopy with and without shaded region (Fig. 10). Though the R^2 (0.0052) between NDVI of canopy without shaded region is greater than with the shaded one, it is still not significant enough to indicate a relationship between NDVI and SWP.

We also analyzed the relationship over a four week time series (Fig. 11). The data of canopy NDVI and SWP within the first, second, third, fourth week were conducted correlation analysis. Among these range levels, the relationship in the range of three weeks is the best, though it is still not strongly correlated for reliably indicating stress.

In summary, practical ground truthing efforts in 2014 growing year have enabled us to conclude that, using a low cost VTOL drone plus COTS RGB/NIR camera pair and performing plain image processing does not lead us to direct correlation to water stress level. However, more recent work (forthcoming) suggests using advanced algorithms based on raw NDVI information can indeed show a correlation to water stress ($R^2 \geq 0.9$).

Acknowledgment

This work is supported in part by UC ANR Competitive Grant Award No. 13-2628 (2014-2019) entitled "Evaluating and extending the use of small, multi-rotor unmanned aerial

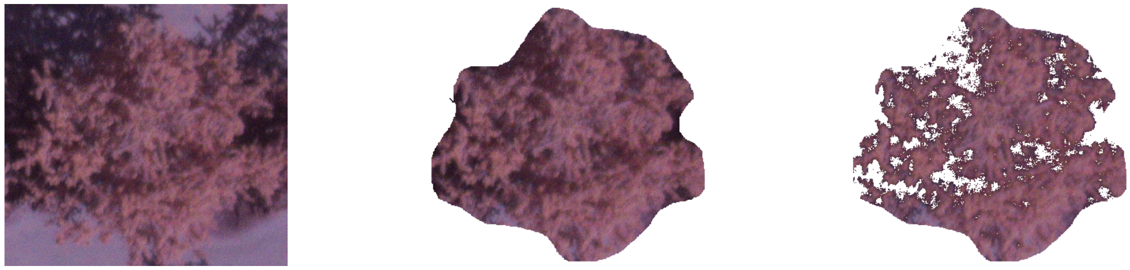

(a) Canopy of a single tree

(b) Canopy of single tree without soil and shade in the background

(c) Canopy of a single tree without shade within it

Fig. 9. Canopy classification

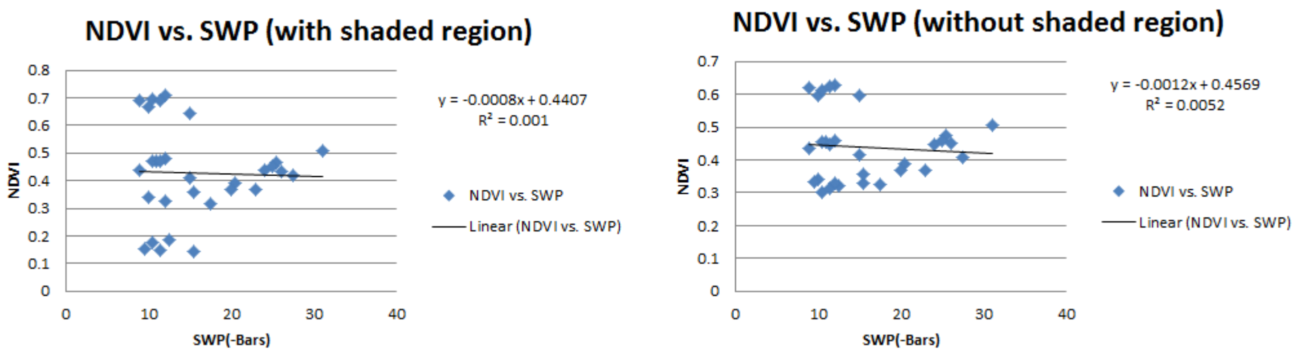

Fig. 10. Correlation analysis between NDVI of canopy without shade and SWP

vehicles (UAV's) as a crop monitoring tool."

The authors would like to thank Larry Burrow for lending his expertise in almond orchard. Thanks go to the MESA Lab Scientific Data Drone crew members Ph.D. student Brendan Smith and Undergraduate Researchers Alejandro Sanchez, Yoni Shchemelinin and Andreas Anderson for contributions in conducting flight missions in the 2014 growing season.

REFERENCES

[1] Slatyer, J. O. (1967). Plant-water relationships. New York and London: Academic Press, 366.

[2] Hsiao, T. C., Fereres, E., Acevedo, E., & Henderson, D. W.. (1976). Water stress and dynamics of growth and yield of crops, water and plant life. Problems and modern approaches: Springer.

[3] Nilsson, H. E. (1995). Remote sensing and image analysis in plant pathology. Canadian Journal of Plant Pathology, 17(2), 154-166.

[4] Castel, J. R., Fereres, E. (1982). Responses of young almond trees to two drought periods in the field. J. Hort. Sci., 57(2), 175–87.

[5] Fereres, E., Goldhamer, D. A.. (1990). Deciduous fruit and nut trees. In: Stewart, B.A.

[6] Hake, S.. (1996). Cotton Production Manual. University of California Division of Agriculture and Natural Resources, Publication 3352, 442.

[7] Micke, W.. (1996). Almond Production Manual. University of California Division of Agriculture and Natural Resources, Publication 3364, 294.

[8] David Doll. (2014). Impact of deficit irrigation on almond kernels. The Almond Doctor (`http://www.thealmonddoctor.com`).

[9] Goldhamer, D. and J. Girona. (2012). Almond. In: P. Steduto, T. Hsiao, E. Fereres, and D. Raes eds. Crop yield response to water. Rome: Food and Agriculture Organization of the United Nations. FAO Irrigation and Drainage Paper 66, 358-373.

[10] Shackel KA, Edstrom J, Fulton A, Lampinen B, Schwankl L. (2011). Drought survival strategies for established almond orchards on shallow soil. Modesto, CA: 2011-2012 annual report to The Almond Board of California.

[11] California breaks drought record as 58% of state hits driest level. (2014). LA TIMES.

[12] Extreme drought in Northern California just got 10% better. (2015). LA TIMES.

[13] Stagakis, S., González-Dugo, V., Cid, P., Guillén−Climent, M. L., & Zarco-Tejada, P. J. (2012). Monitoring water stress and fruit quality in an orange orchard under regulated deficit irrigation using narrow-band structural and physiological remote sensing indices. ISPRS Journal of Photogrammetry and Remote Sensing, 71, 47–61.

[14] Seginer, I., Elster, R. T., Goodrum, J. W., Rieger, M. W.. (1992). Plant wilt detection by computer-vision tracking of leaf tips. Transactions of the ASABE 35(5), 1563–1567.

[15] Peguero-Pina, J. J., Morales, F., Flexas, J., Gil-Pelegrı́n, E., & Moya, I. (2008). Photochemistry, remotely sensed physiological reflectance index and de-epoxidation state of the xanthophyll cycle in Quercus coccifera under intense drought. Oecologia, 156(1), 1-11.

[16] Jones, H. G.. (1999). Use of infrared thermometry for estimation of stomatal conductance as a possible aid to irrigation scheduling. Agric. Forest Meteorol., 95(3), 139-149.

[17] Idso, S.B., Jackson, R.D., Pinter, P.J.J., Reginato, R. J., Hatfield, J. L.. (1981). Normalizing the stress degree-day parameter for environmental variability. Agric. Meteorol.24, 45–55.

[18] Haboudane, D., Miller, J.R., Pattey, E., Zarco-Tejada, P. J., Strachan, I. B.. (2004). Hyperspectral vegetation indices and novel algorithms for predicting green LAI of crop canopies: modeling and validation in the context of precision agriculture. Remote Sensing of Environment, 90(3), 337-352.

[19] Goldhamer, D., & Fereres, E. (2001). Simplified tree water status measurements can aid almond irrigation. California Agriculture, 55(3), 32-37.

[20] Peñuelas, J., Gamon, J. A., Fredeen, A. L., Merino, J., & Field, C. B. (1994). Reflectance indices associated with physiological changes

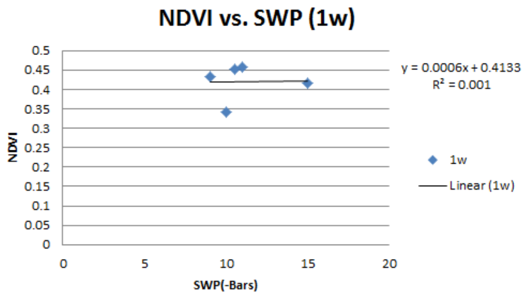

(a) Correlation analysis within 1 week

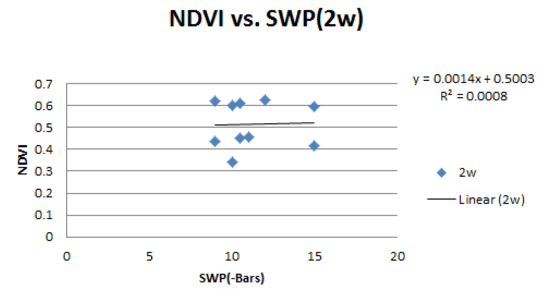

(b) Correlation analysis within 2 weeks

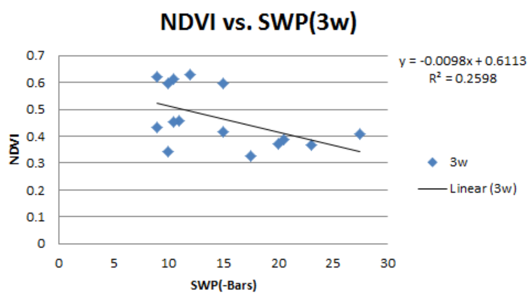

(c) Correlation analysis within 3 weeks

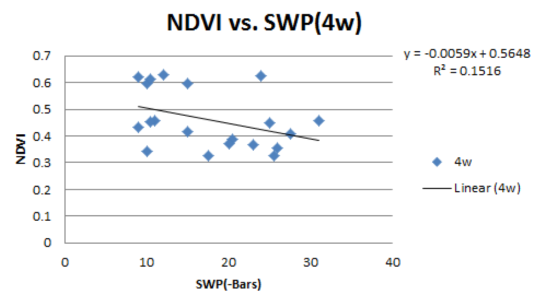

(d) Correlation analysis within 4 weeks

Fig. 11. Correlation analysis with different time range

in nitrogen-and water-limited sunflower leaves. Remote Sensing of Environment, 48(2), 135-146.

[21] Stagakis, S., González-Dugo, V., Cid, P., Guillén-Climent, M. L., & Zarco-Tejada, P. J. (2012). Monitoring water stress and fruit quality in an orange orchard under regulated deficit irrigation using narrow-band structural and physiological remote sensing indices. ISPRS Journal of Photogrammetry and Remote Sensing, 71, 47-61.

[22] Carter, G. A. (1991). Primary and secondary effects of water content on the spectral reflectance of leaves. American Journal of Botany, 916-924.

[23] Gonzalez-Dugo, V., Zarco-Tejada, P., Berni, J. A., Suárez, L., Goldhamer, D., & Fereres, E. (2012). Almond tree canopy temperature reveals intra-crown variability that is water stress-dependent. Agricultural and Forest Meteorology, 154, 156-165.

[24] Suárez, L., Zarco-Tejada, P. J., González-Dugo, V., Berni, J. A. J., Sagardoy, R., Morales, F., & Fereres, E. (2010). Detecting water stress effects on fruit quality in orchards with time-series PRI airborne imagery. Remote Sensing of Environment, 114(2), 286-298.

[25] Berni, J., Zarco-Tejada, P. J., Suárez, L., & Fereres, E. (2009). Thermal and narrowband multispectral remote sensing for vegetation monitoring from an unmanned aerial vehicle. IEEE Transactions on Geoscience and Remote Sensing, 47(3), 722-738.

[26] Smith, G. M., & Milton, E. J. (1999). The use of the empirical line method to calibrate remotely sensed data to reflectance. International Journal of Remote Sensing, 20(13), 2653-2662.

[27] Allen, R. G., Pereira, L. S., Raes, D., & Smith, M. (1998). Crop evapotranspiration-Guidelines for computing crop water requirements-FAO Irrigation and drainage paper 56. FAO, Rome, 300(9).

[28] Fulton, A., J. Grant, R. Buchner, and J. Connell. (2014). Using the pressure chamber for irrigation management in walnut, almond, and prune. Oakland, CA. University of California Division of Agriculture and Natural Resources Publication 8503.